Nonlinear Conversion of Ti: Sapphire Laser Wavelengths

Glen A. Rines, *Member, IEEE*, Henry H. Zenzie, Richard A. Schwarz, *Senior Member, IEEE*, Yelena Isyanova, and Peter F. Moulton, *Senior Member, IEEE*

Invited Paper

***Abstract*— We review a series of experimental investigations into the use of nonlinear optics to shift wavelengths generated by the tunable Ti:sapphire laser. We consider two basic approaches: harmonic generation (and the related process of sum frequency generation) to reach shorter wavelengths, and optical parametric generation to cover longer wavelengths. Both techniques have been aided by the development of two sets of nonlinear crystals, the borates BBO and LBO for harmonic processes, and the KTP family of materials for use with optical parametric generation. In combination we have used nonlinear techniques to produce tunable wavelengths ranging from 193–3000 nm.**

I. Introduction

In terms of frequency coverage, the Ti:sapphire laser is the most widely tunable laser known. The broad gain linewidth is the result of a large shift in lattice position between the two d-level, laser-active electronic states ($^2T_2$ and ^2E in the cubic-field approximation) of the Ti^{3+} ion, combined with a strong Jahn–Teller interaction for both states. Excited-state transitions from the upper laser level are not energetically possible over the region of gain, and thus, the entire emission linewidth is available for laser operation. On the short wavelength end, cw operation at 645 nm has been observed for a system with the laser crystals cooled by liquid nitrogen [1]. At the other extreme, pulsed operation out to 1178 nm has been reported [2]. For practical lasers a good fraction of the maximum power can be generated over the tuning range 700–1000 nm, which represents, in frequency, a span of nearly 4300 cm^{-1}.

The Ti:sapphire tuning range covers the bandgaps of several technologically important III–V and II–VI semiconductors, a number of rare earth and metal vapor transitions, the region of highest human tissue transparency, and the weak absorption transitions of water vapor and oxygen. The latter are of use in atmospheric remote sensing. If the tunable output of the Ti:sapphire can be shifted to shorter wavelengths, however, a wider variety of applications becomes possible. Shorter wavelengths access the intense UV electronic transitions of atoms and molecules, the bandgaps of widegap semiconductors, and some dielectrics and metals, the region of maximum liquid-water transparency, and blue wavelengths useful for color projection. Wavelengths longer than the Ti:sapphire fundamental cover those used for fiber communications, resonate with a variety of vibrational rotational molecular transitions, and are more eye safe—an important consideration for atmospheric measurement applications.

We have previously reported on the operation of high-energy, Ti:sapphire lasers pumped by frequency-doubled, Q-switched, pulsed, Nd-doped solid-state lasers [3], [4]. The operating characteristics of these systems are now well known and are similar in many ways to Q-switched, Nd-doped lasers, but with broadly tunable output. Commercial devices are available with output energies on the order of 100 mJ. With the use of unstable-resonator cavities, laser-pumped Ti:sapphire lasers can produce near-diffraction-limited output beams, ideal for driving nonlinear processes. Below, we briefly review the important properties of unstable resonator-oscillators, with and without injection seeding. Following this, we discuss our recent work with frequency conversion processes, considering first techniques to shift to shorter wavelengths, and then covering the use of optical parametric generation to produce longer wavelengths.

II. Properties of the Ti: Sapphire Laser

In all of the frequency conversion experiments described in this paper, the fundamental is obtained from a Ti:sapphire, unstable resonator-oscillator, with a graded-reflectivity-mirror (GRM) output coupler. This resonator design, first reported in [4], provides a near-diffraction-limited spatial beam with a Gaussian intensity distribution. The spectral linewidth is on the order of 1 nm (FWHM) when operated without injection seeding. When injection-seeded with a single frequency cw source, the linewidth is within two to three times the transform limit (<1 pm). We have carried out nonlinear conversion experiments, with and without injection seeding of the oscillator. In all cases, the seeded oscillator produces a symmetric output beam with an M^2 of about 1.1. In contrast, the unseeded oscillator produces a slightly asymmetric output beam with an M^2 of about 1.2 in the plane perpendicular to the electric field polarization, and about two in the plane parallel to the polarization. The increase in M^2 in the parallel plane results from the presence of intracavity prisms combined with the 1-nm linewidth.

Manuscript received December 2, 1994; revised December 7, 1994. This work was supported by projects under ARPA, NASA, NIH, NSF, and internal company R&D funds. Most of the projects were part of the Small Business Innovative Research Program.

The authors are with Schwartz Electro-Optics, Inc., 45 Winthrop Street, Concord, MA 01742 USA.

IEEE Log Number 9409718.

1077–260X/95$04.00 © 1995 IEEE

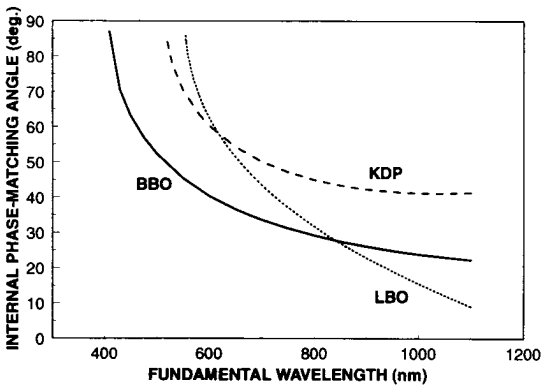

Fig. 1. Type I SHG phasematching angle as a function of wavelength for three crystals at room temperature.

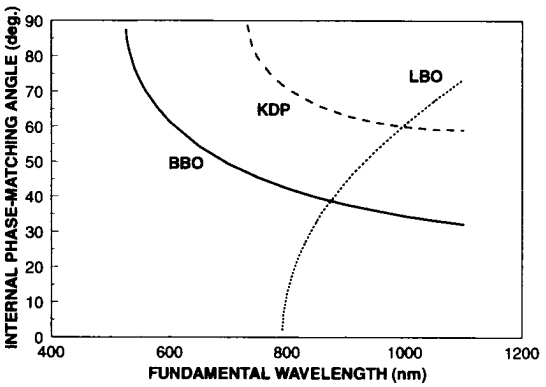

Fig. 2. Type II SHG phasematching angle as a function of wavelength for three crystals at room temperature.

In some of the experiments discussed below, we employed an oscillator that operated with a maximum energy of 100-mJ, with nominal beam diameter of 2 mm $(1/e^2)$ and a FWHM pulsewidth of 10 ns (17 ns $1/e^2$) at the gain peak of 800 nm. We also report on experiments with an oscillator designed for higher pump energies, capable of providing up to 400 mJ with a nominal beam size of 3.5 mm $(1/e^2)$ and a 8-ns FWHM pulsewidth (14 ns $1/e^2$).

III. Second Harmonic Generation

There are a variety of nonlinear crystals that can be phase-matched for second harmonic generation (SHG) of at least some fraction of the Ti:sapphire tuning range. There are three crystals that can be phasematched for SHG over the entire Ti:sapphire tuning range and, in addition, have the broad transparency and high damage resistance needed for use with the high peak-power, pulsed Ti:sapphire laser: KH_2PO_4 (KDP), β-Ba_2BO_4 (BBO) and LiB_3O_5 (LBO). We have carried out SHG experiments with all three of these crystals, and obtained efficient, optical-damage-free conversion.

Figs. 1 and 2 show the type I and II, respectively, phase-matching angles over the 400- to 1100-nm fundamental wavelength region for the three materials, at room temperature. For all cases, except type I KDP SHG, the effective nonlinearities vanish at the short wavelength limits. In Table I, we list the important nonlinear properties of the crystals for both type I and type II configurations, listed in order of increasing power threshold. The latter is a figure of merit for nonlinear harmonic conversion, first defined by Eimerl [5]. The notation in the Table describes the specific crystal angle varied in Figs. 1 and 2, where we have used the conventions established by Roberts [6]. We present values in the Table at several specific wavelengths for each crystal/type combination, to indicate the variation that occurs over some of the Ti:sapphire tuning range.

TABLE I
Computed NLO Characteristics of Candidate Crystals for SHG of 700-940 nm @ 25°C Using Physical Data, Definitions, Conventions and Reference Frames in [6]

Crystal Configuration	Fund. λ (nm)	θ (degrees)	φ (degrees)	Walkoff ρ_1 (mrads)	Walkoff ρ_2 (mrads)	Walkoff ρ_3 (mrads)	d eff. (pm/V)	d^2/n^3 (pm^2/V^2)	Ext. P_{av} (MW)	L*dA (cm-mr)	L*dT HWHM (cm-°C)	L*dλ (cm-nm)
LBO	700	--	--	--	--	--	--	--	--	--	--	--
Type-II	860	90	35.6	0	9	0	0.41	0.042	1.9	4.24	4.5	0.61
(neg.)	911	90	46.5	0	9	0	0.50	0.063	1.6	4.27	3.5	0.83
	940	90	51.6	0	9	0	0.54	0.072	1.4	4.53	3.3	0.99
LBO	700	43.4	0	0	0	19	0.66	0.102	9.2	0.82	41.8	0.20
Type-I	860	26.1	0	0	0	14	0.79	0.148	5.5	1.32	1.8	0.55
(neg.)	911	21.9	0	0	0	13	0.80	0.155	4.5	1.60	1.9	0.74
	940	19.8	0	0	0	12	0.81	0.159	3.9	1.81	2.1	0.88
BBO	700	49.4	0,60	71	0	77	0.89	0.183	25	0.37	4.9	0.15
Type-II	860	39.3	0,60	72	0	75	1.26	0.363	17	0.48	8.5	0.37
(neg.)	911	37.2	0,60	71	0	74	1.33	0.406	16	0.52	9.9	0.49
	940	36.2	0,60	70	0	73	1.37	0.422	16	0.54	10.7	0.57
BBO	700	33.7	90	0	0	75	2.06	0.921	16	0.21	4.7	0.13
Type-I	860	27.2	90	0	0	64	2.11	0.974	17	0.30	8.5	0.34
(neg.)	911	25.8	90	0	0	62	2.11	0.980	17	0.33	9.8	0.45
	940	25.1	90	0	0	60	2.11	0.982	17	0.34	10.6	0.52
KDP	700	--	--	--	--	--	--	--	--	--	--	--
Type-II	860	65.5	0,90	19	0	22	0.30	0.027	22	1.55	4.7	0.88
(neg.)	911	62.7	0,90	20	0	23	0.32	0.031	25	1.52	5.2	1.31
	940	61.5	0,90	20	0	24	0.33	0.032	27	1.52	5.5	1.69
KDP	700	50.2	45	0	0	29	0.34	0.033	69	0.53	3.0	0.28
Type-I	860	43.1	45	0	0	29	0.29	0.024	136	0.65	4.6	1.02
(neg.)	911	42.1	45	0	0	29	0.28	0.023	158	0.70	5.0	1.70
	940	41.7	45	0	0	29	0.28	0.023	170	0.73	5.2	2.42

The majority of our experimental effort involved the use of BBO. The available physical size of BBO material, and the relatively small change in phasematching angle with wavelength, allows one crystal to be used over the entire Ti:sapphire tuning range, a valuable property in many applications. One BBO crystal with a 6-mm aperture and a 2-mm input beam diameter can be angle-tuned over the entire 700–1000-nm tuning range. The concomitant penalty of a narrow angular acceptance angle requires low-divergence fundamental beams for efficient SHG. On the other hand, at the crystal lengths used in our work, BBO has by far the largest temperature acceptance range, approximately 20 C.

The well-known KDP crystal has a high threshold power in the type I configuration, and the beam sizes we used require long crystal lengths (30 mm) for optimum conversion. In one experiment, with a 15-mm–long KDP(I) system and the high-energy oscillator at 790 nm, we obtained 31% conversion efficiency at 190 mJ of input. With a 6-mm–long BBO(I) crystal, the efficiency was nearly twice that level. If we were to optimize the KDP(I) SHG configuration by using longer length (30 mm) crystals, a crystal of 12 mm aperture would be required for full wavelength coverage over the Ti:sapphire tuning range, the temperature acceptance would be only 2 C,

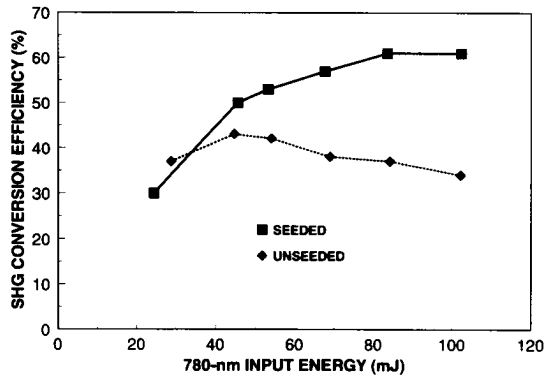

Fig. 3. BBO SHG conversion efficiency as a function of 780-nm input energy for both unseeded and seeded Ti:sapphire lasers.

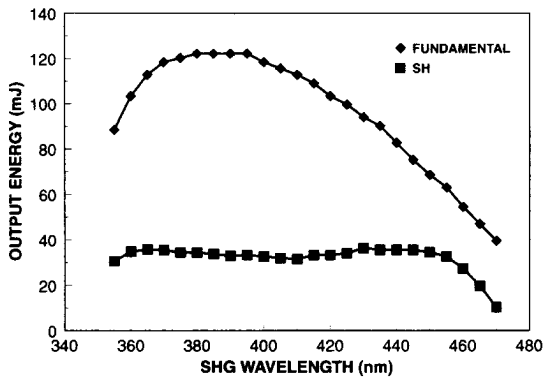

Fig. 4. Fundamental and second-harmonic output energy as a function of harmonic wavelength for the (nominal) 100-mJ Ti:sapphire laser and BBO crystal.

and the limiting efficiency would be expected to be only about half that of BBO(I) for our laser sources. Using a 25-mm-long KDP(II) crystal, we observed 25% conversion for 100 mJ of input at 911 nm, compared to 41% conversion for a 6-mm BBO crystal with the same input. As with KDP(I), an optimized KDP(II) SHG configuration would have a relatively narrow temperature acceptance, would need an even larger aperture to cover the Ti:sapphire range, and, from Fig. 2, would not phasematch below a wavelength of 730 nm.

LBO has the lowest power threshold, a high surface-damage threshold and, unlike BBO and KDP, the material is nonhygroscopic. The crystal is known to be capable of operation at high average powers. For example, in unrelated studies, we have generated 60 W of average second-harmonic power with a Nd:YAG laser drive source. A practical problem for LBO, at present, is the limited size of high-quality single crystals. Because of this, we did not attempt to obtain data for the LBO(II) configuration, which achieves efficient conversion only with crystal lengths of 30–50 mm, a size not available for our studies. Another problem with LBO(II) is, from Fig. 2, the short wavelength cutoff of 792 nm for room-temperature material. Previous work, with a 5-mm–thick LBO(I) crystal and a pulsed Ti:sapphire laser, showed 20–30% conversion efficiencies over a 700–900-nm fundamental region, for input pulse energies in the 20–30 mJ range [7]. Below, we show data comparing LBO(I) and BBO(I) with our high-energy Ti:sapphire source.

Fig. 3 shows the typical SHG conversion efficiency that we observe when using the 100-mJ scale oscillator, with a BBO(I) crystal of nominally optimum length (6 mm) for the 2-mm diameter $(1/e^2)$ beam. The graph includes data for the seeded and unseeded oscillator. The lower saturated efficiency for the unseeded case is due to two factors. First, the nominal 1-nm linewidth exceeds the spectral acceptance of 0.5 nm for a 6-mm crystal. Second, the unseeded beam is slightly larger in diameter and divergence in one plane, which amounts to lower drive and higher dephasing. Perhaps the most striking result of this experiment is that we reach what appears to be a saturating conversion efficiency with an input peak power of <6 MW (100 mJ, 17 ns $1/e^2$ width) when the calculated power threshold listed in Table I is 17 MW.

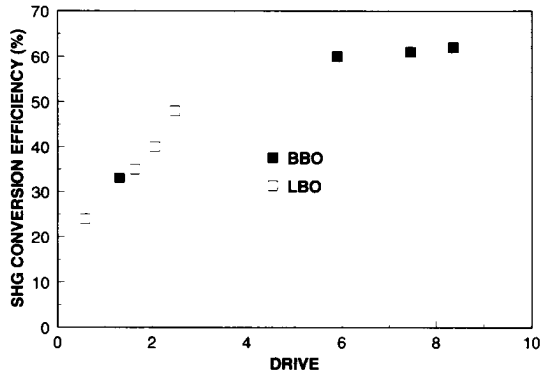

Fig. 5. SHG conversion efficiency as a function of nonlinear drive for BBO and LBO crystals.

Fig. 4 shows tuning data for the nominal 100-mJ oscillator, with both the fundamental and second harmonic pulse energies plotted. The unseeded SHG conversion efficiency data in Fig. 3 can be used as reference when analyzing the shape of the tuning curve in Fig. 4. That is, the sharp drop in the SHG energy at the endpoints is directly related to the lower energy provided by the oscillator in these regions. Also, the flatness of the central portion of the SHG curve corresponds to the saturated portion of the unseeded SHG conversion curve.

We took the remainder of the SHG data presented here with the larger Ti:sapphire oscillator. The maximum peak power is about 30 MW in the average intensity terms used by Eimerl [5] for the power threshold definition. Fig. 5 shows a comparison of SHG conversion efficiency as a function of nonlinear drive for 10-mm LBO(I) and 6-mm BBO(I) crystals. The BBO crystal has been taken to a nonlinear drive of greater than eight, and the conversion efficiency has clearly saturated. By comparison, the LBO crystal, being shorter than optimum length for this input beam, has not reached a saturated efficiency. An optimum-length LBO crystal, nominally 20 mm for the large Ti:sapphire laser beam, shows promise for exceeding the 60% conversion level reached by the 6-mm BBO crystal.

Based on the theory of Cousins [8] for Gaussian beams in time and space, we would expect the SHG efficiency in general to saturate at the 90% level for a dephasing parameter, $\delta = 0$ and at slightly less than 40% for $\delta = 1$. For our

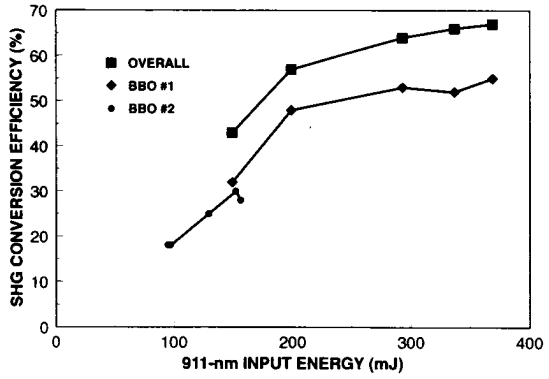

Fig. 6. SHG conversion efficiency as a function of fundamental energy at 911 nm for a two-BBO-crystal scheme. BBO #1 is data for the first crystal, and BBO #2 is data for the second crystal, driven by the unconverted fundamental existing from the first crystal. The overall conversion is shown as the sum of the outputs from both crystals divided by the input energy to the first crystal.

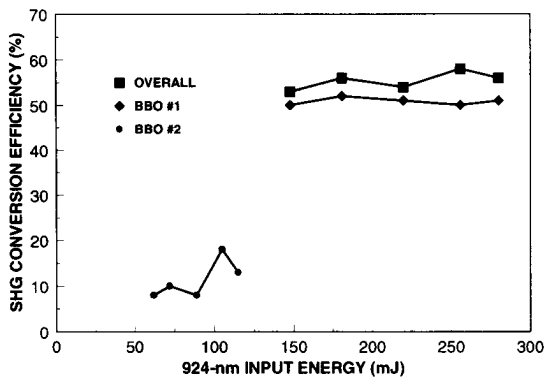

Fig. 7. Similar to Fig. 6, but for a quadrature scheme for two BBO crystals, where the total SHG output appears in one beam. The fundamental wavelength is 924 nm.

BBO data, we thus conclude that the dephasing parameter was somewhat less than unity. One possible cause of the dephasing was imperfect collimation of the unstable resonator output beam, and correction of this may lead to enhanced SHG from Ti:sapphire lasers in future experiments.

We performed some preliminary investigations of two crystal SHG schemes with BBO(I) crystals. Data from these preliminary tests are presented in Figs. 6 and 7. Fig. 6 shows the results from a simple parallel-crystal arrangement. In this experiment, using a fused silica dispersing prism, we separated the unconverted fundamental from the second-harmonic, after the beam exited the first SHG crystal. We then sent the residual fundamental beam through a second 6-mm, BBO(I) crystal. Fig. 6 shows the SHG conversion as a function of the fundamental energy present in each individual crystal. It also shows the conversion, for the sum of the two SHG outputs, as a function of the total fundamental used as the input to the two-crystal configuration. The overall conversion of 67% of the fundamental to second harmonic in this experiment is the best SHG conversion we have obtained to date, and has resulted in the highest SHG pulse energy, 250 mJ. The 67% level is an external conversion-efficiency value, that is, second harmonic energy exiting the crystal configuration divided by the total fundamental output from the oscillator. Both BBO crystals were 6 mm long and had broadband solgel AR coatings on both surfaces.

Fig. 7 shows data from a type I quadrature SHG experiment we carried out, with the same two BBO crystals used in the parallel scheme. In this configuration, a single beam line is maintained for a two-crystal arrangement, which is generally more useful than the parallel scheme, discussed above. With type I SHG, the fundamental and second harmonic generated are orthogonally polarized. The output from the first SHG crystal can be prepared for a second quadrature crystal by passing the beam though an optical rotator cut such that the fundamental and second harmonic polarizations are made parallel. We achieved this for the 924/462 nm case by using a 3.04-mm–thick quartz rotator. The second BBO(I) crystal was oriented so that the fundamental polarization was correctly aligned for phasematching. The second harmonic polarization remains orthogonal to the phasematching plane, hence, there is no back conversion of harmonic energy produced in the first crystal. As with the parallel-crystal data, we show conversion efficiency as a function of the fundamental energy available to each crystal individually, as well as the total conversion value.

In both of these two dual-crystal experiments, an incremental improvement in efficiency was obtained. Further improvement should be possible by optimizing crystal lengths for each stage, as discussed by Eimerl [5].

IV. Third Harmonic Generation

We have done all of our THG experiments with BBO crystals, and have tested both type I and type II configurations. A type II THG crystal following a type I SHG crystal is advantageous, because the orthogonal polarization states exiting the SHG stage are correctly oriented for the type II mixing process in the THG crystal. To use a type I THG stage, one must rotate the polarizations of the fundamental and second harmonic, such that the two are parallel. This requires a rotator, such as the one described above in the type I quadrature SHG experiment. Since achromatic rotators are not readily available, this is a serious complication for tunable systems.

With the type II THG configuration, angle tuning over about 30° (internal angle) is required to cover the 700–950-nm fundamental tuning range. We have demonstrated THG operation tuning the fundamental from 720–930 nm, using a single SHG crystal and two THG crystals to cover the angle tuning range.

With unseeded oscillator inputs, we have seen THG conversion efficiencies of 1–10%. Seeding leads to higher SHG conversion and, subsequently, higher overall THG conversion; we have observed efficiencies as high as 21%.

Table II lists highlights of our THG experiments, showing not only the highest pulse energies that we have achieved, but a single-point comparison between type I and type II THG, at 924 nm. For the conditions in this one-point comparison, the type I THG shows significantly higher conversion efficiency. No attempt was made, however, to optimize THG crystal lengths in this work. Owing to its simplicity, the type II

TABLE II
COMPARISON OF TYPE I AND TYPE II THG IN BBO AT 924 nm

	BBO Type I		BBO Type II	
	Internal Conversion Efficiency	THG Energy Obtained	Internal Conversion Efficiency	THG Energy Obtained
Unseeded	14%	19 mJ	13%	20 mJ
Seeded (SLM)	33%	35 mJ	16%	20 mJ

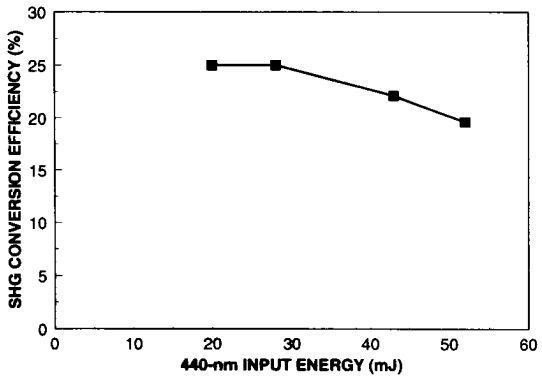

Fig. 8. Conversion efficiency as a function of 440-nm input energy for the BBO second stage of a Ti:sapphire, fourth-harmonic-generation scheme.

approach merits further effort in optimization, particularly for tunable systems. Both of the high-energy points were limited by damage to the exit face of the BBO THG crystal. Future THG optimization work should concentrate on beam shaping, to raise efficiency while minimizing exit face fluences.

V. FOURTH HARMONIC GENERATION

BBO(I) can phase match for SHG with a fundamental input as short as 410 nm. Hence, a pair of BBO(I) crystals can provide, in principle, the fourth harmonic of the fundamental Ti:sapphire laser to a short wavelength limit of 205 nm. As we noted above, the angular dependence of the nonlinear coefficient for BBO leads to a vanishing nonlinear interaction as 410-nm SHG is approached and thus, the effective short wavelength limit is somewhat longer. We have obtained measurable FHG output at wavelengths as short as 207 nm. The best conversion efficiency we obtained to date is shown in Fig. 8, for a 220-nm output wavelength. We took the data with the larger Ti:sapphire oscillator, but limited the 440-nm input to the second doubling crystal to 50 mJ. The last point on the curve corresponds to 10 mJ of energy. The conversion efficiency in this experiment saturated at 25%, and decreased as the input energy was further increased. Nonlinear UV absorption has been observed in BBO, and we believe that the relatively low conversion efficiency was, in part, the result of this effect.

VI. DEEP UV GENERATION VIA SUM FREQUENCY MIXING

Sum frequency mixing (SFM) of a pulsed Ti:sapphire laser and a Q-switched Nd:YAG laser has been used previously to generate over 350 mJ of 457-nm energy [9]. In our work, we have used SFM as a means to produce wavelengths below 200 nm.

TABLE III
DEEP UV OUTPUT DATA AT λ_{SFM} = 195.4 nm

Fundamental Ti:S input energy (ω):	165 mJ
Total SHG produced (2ω):	26 mJ (16 % SHG conversion)*
Total FHG produced (4ω):	3.6 mJ (14 % FHG conversion)
Total OPO idler output produced:	5.8 mJ
FHG input to SFM crystal:	3.4 mJ
Idler input to SFM crystal:	3.3 mJ
Total SFM produced:	1.8 mJ (27 % SFM conversion)
SFM Output Pulsewidth:	~5 ns FWHM

* Deliberately de-optimized to provide sufficient residual fundamental energy.

Historically, it has been difficult to produce tunable, coherent radiation in the ultraviolet region of the spectrum, below 200 nm. This is due, in part, to the limited number of usable fundamental laser transitions in the UV. Dye lasers can provide broadly tunable radiation in the visible/near-UV region and, with harmonic generation in nonlinear crystals, this translates into potential tunability in the UV. However, nonlinear crystals that meet all the requirements for phasematched UV generation below 200 nm have not been readily available. BBO has been used in a SFM configuration to generate cw 194-nm output, by combining a Ti:sapphire laser, with the 257-nm output of a frequency-doubled, Ar–ion laser [10]. In order to avoid the limitation of crystals, one can resort to higher order processes in gases, such as four wave mixing. A Ti:sapphire-based source has been used for the generation of 130 nm energy in Hg vapor [11]. In recent experiments, we have shown that LBO can be used with SFM to convert tunable Ti:sapphire laser radiation to tunable UV below 200 nm. Details of this work will be published separately. Here, we present a summary of the approach and results.

Our scheme is based on SFM, in an LBO crystal, of UV energy in the 205–230 nm region with infrared energy in the 1700–2500 nm region. This method exploits the broad UV transparency of LBO, which transmits wavelengths as short as 160 nm, and has been discussed in theory [12]. The fourth harmonic of the Ti:sapphire laser provides the 205–230 nm UV source. Some of the Ti:sapphire laser output in the fundamental is used to pump a $KTiOPO_4$(KTP) OPO, whose idler output provides the infrared source. LBO can be phasematched in both the type I and type II configurations for this process. The deep UV output is tunable by tuning the Ti:sapphire laser wavelength and the OPO idler wavelength.

In our initial experimental work, we successfully demonstrated the LBO sum-frequency-mixing scheme with a temperature tuned, noncritically-phasematched, 15-mm–long, type II configuration. We generated $\geq$0.4 mJ of 10-Hz tunable UV output in the wavelength range 194.6–196.1 nm, with a maximum demonstrated energy of 1.8 mJ at 195.4 nm, and measured conversion efficiencies as high as 27%. We also generated a small amount of output at wavelengths as short as 193.0 nm, where the limits of our LBO temperature tuning hardware prevented operation at higher powers. These results were all obtained with $<$170 mJ of total fundamental titanium-sapphire energy. Table III lists the output energies generated at each of the intermediate wavelengths generated for the high-energy point at 195.4 nm.

While the tuning in this initial experiment was limited to 3 nm in the UV, we estimate that we will be able to tune from 187–207 nm with an angle-tuned LBO crystal.

VII. Parametric Generation

Parametric generation, the inverse of harmonic generation, shifts the energy output of the input (pump) source to energy in signal and idler outputs at longer wavelengths. The nonlinear crystal employed can be adjusted in temperature and/or angle to vary the signal and idler wavelength, providing a tunable source even when the pump wavelength is fixed. Thus, the tunability of the Ti:sapphire laser would appear to be of little use when the device pumps the most common parametric generator, the optical parametric oscillator (OPO).

We have recently reported [13] on one case, where tuning the OPO pump source does provide an advantage. For the nonlinear material KTP it is possible to maintain type II, noncritical phasematching (NCPM) for pump wavelengths over the entire tuning range of the Ti:sapphire laser. Thus, the advantages of NCPM operation, which include the absence of walkoff, broad angular and spectral acceptance, and for the type II matching condition in KTP, a narrow OPO gain linewidth, can be realized for a wide range of signal and idler wavelengths. In the reported work, we were able to generate NCPM signal and idler wavelengths from 1.03–1.28 μm and from 2.18–3.03 μm, as the pump tuned from 700–900 nm. At a pump wavelength of 760 nm, we generated 49 mJ of combined signal and idler energy for a pump energy of 110 mJ and observed a conversion slope efficiency of 55%. We also reported on an OPO based on angle matched $KNbO_3$, in which we observed degenerate operation over a pump wavelength range of 720–818 nm.

We report here on two new, nanosecond Ti:sapphire-pumped OPO's, which are based on two isomorphs of KTP, $K(TiO)AsO_4$ (KTA) and $Cs(TiO)AsO_4$ (CTA). The two isomorphs have previously been operated in OPO's, pumped by a femtosecond Ti:sapphire laser [14], [15]. Both crystals transmit further into the IR than KTP, and in the case of CTA have significantly different phasematching characteristics. In our experiments the KTA crystal, provided by Crystal Associates (Waldwick, NJ), was 15 mm long, with antireflection (1.05–1.25-μm band) coatings on the 5 × 5 mm faces. The CTA crystal, provided by L. K. Cheng, at DuPont Central Research (Wilmington, DE), was 22 mm long, with no AR coating on the 6 × 7 mm faces. Both crystals were oriented for the type II configuration, "x-cut," in which the pump and signal are polarized parallel to the y-axis and the idler is polarized parallel to the z-axis: all beams propagate along the x-axis. The OPO cavity designs were simple two-mirror, standing-wave resonators. The input mirrors were coated for nominally high transmission at the pump wavelength, and high reflection at the signal wavelength. The output mirror, which was partially transmitting at the signal wavelength, was coated to highly reflect the pump wavelength, in order to reduce the OPO threshold by double passing the pump beam through the crystal. Two sets of mirrors were used in our experiments: one set for the KTA-based OPO, and another for the CTA-based OPO. Our pump laser was the 100–mJ oscillator, operating without injection-seeding.

TABLE IV
Parameters and Threshold of KTA OPO at Three Pump Wavelengths

Wavelength		Input mirror	Output mirror	Threshold	
Pump (nm)	Signal (nm)	Pump transmission (%)	Signal reflection (%)	Observed (mJ)	Calculated (mJ)
724	1090	87	43.5	10.5	10.8
775	1124	85	29.3	15	17.6
852	1207	82	29.0	23	22.7

The KTA OPO resonator had mirrors spaced 5 cm apart, with a flat input mirror and a 7-m–radius output mirror. We generated the KTA OPO signal within the range 1.09–1.239 μm, by tuning the Ti:sapphire laser from 724 to 874 nm. The OPO tuning beyond 1.239 μm was limited, because of the combined effects of a reduced energy available from the pump laser and a low reflectivity from the output mirror. The signal wavelengths were somewhat longer than those predicted by the most recently reported Sellmeier coefficients for KTA [16]. The discrepancy reduced gradually from 10 to 2–3 nm as the pump wavelength increased. The difference may be the result of slight index variations in KTA crystals grown with different levels of impurities.

The signal wavelength range 1.09–1.239 μm corresponds to an idler tuning range of 2.156–2.967 μm. The observed and calculated energy thresholds for the KTA crystal, as well as the input-mirror pump transmission and output-coupler transmission data, are listed in Table IV for three pump wavelengths. We based our calculated thresholds on the theory of Brosnan and Byer [17], pump and signal spot sizes of 0.1 and 0.025 cm, a pump pulse duration of 20 ns (FWHM), appropriate for the pump laser at low energies, and an effective pump reflection of 90% from the output coupler. We assumed that the nonlinearity of KTA is the same as KTP. The excellent agreement between calculated and observed thresholds may be fortuitous, given uncertainties in key parameters, such as the pump spot size.

The energy input-output relation for the same three pump wavelengths is shown in Fig. 9, where the total (signal and idler) output energy is plotted as a function of pump energy incident on the OPO cavity. The slope efficiency is similar for all wavelengths, in the range 40–55%. With the pump-transmission loss (10–20%) of the input mirror accounted for, the maximum slope efficiency for incident pump power on the crystal is over 60%, essentially the same as we found in previous work with KTP.

The CTA crystal [18] is at an early stage of development compared to the other materials, and crystal purity is an issue. The OPO crystal we used had noticeable flaws. Internal damage sites developed during OPO operation, which limited our ability to take reproducible input-output data. The OPO cavity consisted of two flat mirrors spaced 3.5 cm apart. The output-mirror reflectivity for the signal wavelength was low, approximately 15% in the 1.5–1.6-μm wavelength region. Threshold pump energies fell in the range 25–30 mJ for all pump wavelengths. When tuning the Ti:sapphire laser from 714–901 nm, we obtained a signal output from 1.587–1.617 μm, with a

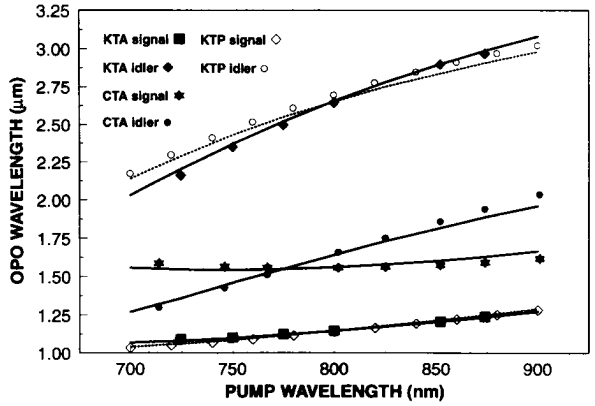

Fig. 9. Total KTA OPO output energy as a function of the pump energy at different signal wavelengths. The threshold points shown are extrapolated from the input-output data.

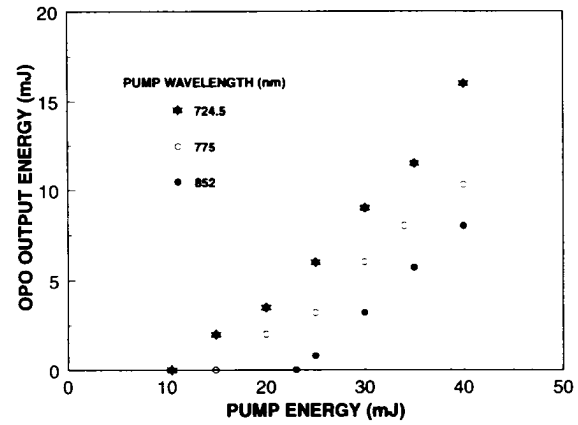

Fig. 10. Signal and idler wavelengths versus pump wavelength for KTP, KTA, and CTA OPO's. The points plotted are data, and the lines are theoretical predictions. The lines for KTP signal and ideal are dotted to distinguish them from KTA theory.

minimum at 1.557 μm. The corresponding idler tuning range is 1.297–2.034 μm. We tested the idler wavelength at several pump wavelengths and found a good agreement with the expected value. For CTA the idler output (polarized parallel to the z axis) is shorter in wavelength than the signal at short pump wavelengths. The degenerate operating point occurred at a pump wavelength of approximately 775 nm.

In Fig. 10 we plot tuning results on all our Ti:sapphire-pumped KTP and isomorph OPO's, to date. Included in the figure are experimental data (points) on signal and idler wavelengths as a function of pump wavelength for KTP, KTA, and CTA crystals. The continuous curves are theoretical calculations, based on coefficients from Kato and Masutani [19], Fenimore *et al.* [16], and Cheng *et al.* [20] for KTP, KTA, and CTA, respectively. The match is good in all cases.[1]

As Fig. 10 shows, the use of KTP and isomorph crystals in OPO's pumped by the Ti:sapphire laser results in NCPM generation of wavelengths providing almost complete coverage of the 1–3 μm region. We have also calculated tuning data for "y-cut" crystals, where the pump and signal are polarized along the x-axis and the idler is polarized along the z-axis. For that case the wavelength coverage is similar to that with "x-cut" crystals, but the gap between signal and idler wavelengths is increased. This is particularly true for CTA, where we predict that there is no degenerate operating point over the range of Ti:sapphire pump wavelengths.

The development of Ti:sapphire-pumped OPO's is still in the early stages. At this writing damage-free and high-efficiency operation with good quality crystals has been demonstrated. Characterization of the signal and idler beam quality and linewidth remain to be done, and techniques for improving beam quality and reducing linewidth to meet various application requirements will need to be examined. Although we have demonstrated operation with NCPM only, the use of angle tuning is certainly possible to provide additional flexibility in wavelength coverage, with the resultant need for tighter requirements on pump-beam quality and crystal alignment.

VIII. Summary

The pulsed, gain-switched Ti:sapphire laser, pumped by a Q-switched, frequency-doubled Nd:YAG laser, and operated with an appropriate cavity to produce a near-diffraction-limited beam, is a suitable drive source for a number of efficient, nonlinear processes, including harmonic, sum-frequency and parametric generation. As a drive source, it is similar to high-beam-quality, Q-switched Nd:YAG lasers, but has the added flexibility of a broadly tunable output. The extended frequency coverage afforded by nonlinear conversion techniques allows Ti:sapphire laser systems to be placed in a widened variety of applications.

Acknowledgment

We gratefully acknowledge D. Roberts and G. C. Catella, of Cleveland Crystals Inc., for their assistance in calculating nonlinear properties of the SHG crystals.

References

[1] Isaac Bass, Lawrence Livermore Laboratory, Livermore, CA, private communication.
[2] L. G. Deshazer and K. W. Kangas, "Extended infrared operation of a titanium sapphire laser," in *Conf. Lasers Electro-Opt. Tech. Dig. Ser.*, Washington, DC, Opt. Soc. Am., vol. 14, pp. 296–298, 1987.
[3] G. A. Rines, P. F. Moulton, and J. Harrison, "Narrowband, high energy Ti:Al_2O_3 lidar transmitter for spacecraft sensing," in *Proc. OSA Topical Meeting on Tunable Solid-State Lasers*, May 1–3, Cape Cod, MA, 1989.
[4] G. A. Rines and P. F. Moulton, "Performance of gain switched Ti:Al_2O_3 unstable resonator lasers," *Opt. Lett.*, vol. 15, pp. 434–436, 1990.
[5] D. Eimerl, "Quadrature frequency conversion," *J. Quantum Electron.*, vol. QE-23, pp. 1361–1371, 1987.
[6] D. A. Roberts, "Simplified characterization of uniaxial and biaxial nonlinear optical crystals: A plea for standardization of nomenclature and conventions," *J. Quantum Electron.*, vol. 28, pp. 2057–2074, 1992.
[7] G. A. Skripko, S. G. Bartoshevich, I. V. Mikhnyuk, and I. G. Tarazevich, "LiB_3O_5: A highly efficient frequency converter for Ti:sapphire lasers," *Opt. Lett.*, vol. 16, pp. 1726–1728, 1991.
[8] A. K. Cousins, "Power conversion efficiency in second harmonic generation with nonuniform beams," *J. Quantum Electron.*, vol. 29, pp. 217–226, 1993.

[1] In a separate experiment, we observed CTA OPO operation with a 1.064-μm, Nd:YAG pump. The observed signal wavelength, 1.86 μm, was not in good agreement with the predicted value of 2.00 μm. The Sellmeir coefficients for CTA were derived by DuPont through measurements limited to wavelengths shorter than 1.5 μm. This is a likely explanation for the large discrepancy between theory and experiment for the Nd:YAG pump source.

[9] A. J. Brown, C. H. Fisher, and K. Kangas, "Efficient, high energy, narrow band, blue light source," *Opt. Lett.*, vol. 18, pp. 1177–1179, 1993.
[10] M. Watanabe, K. Hayasaka, H. Imajo, and Shinji Urabe, "Continuous wave sum frequency generation near 194 nm in β-BaB_2O_4 crystals with an enhancement cavity," *Opt. Lett.*, vol. 17, pp. 46–48, 1992.
[11] C. H. Muller, III, D. D. Lowenthal, M. A. DeFaccio, and A. V. Smith, "High efficiency, energy scalable, coherent 130-nm source by four wave mixing in Hg vapor," *Opt. Lett.*, vol. 13, pp. 651–653, 1988.
[12] J. T. Lin and K. Kato, "Generation of deep UV sources (160–250 nm) by frequency mixing in Lithium-triborate (LBO) crystal," *SPIE*, vol. 1220, Nonlin. Opt., pp. 58–63, 1990.
[13] H. H. Zenzie and P. F. Moulton, "Tunable optical parametric oscillators pumped by Ti:sapphire lasers," *Opt. Lett.*, vol. 19, pp. 963–965, 1994.
[14] P. E. Powers, S. Ramakrishna, C. L. Tang, and L. K. Cheng, "Optical parametric oscillation with $KTiOAsO_4$," *Opt. Lett.*, vol. 18, pp. 1171–1173, 1993.
[15] P. E. Powers, C. L. Tang, and L. K. Cheng, "High repetition rate femtosecond optical parametric oscillator based on $CTiOAsO_4$," *Opt. Lett.*, vol. 19, pp. 37–39, 1994.
[16] D. L. Fenimore, K. L. Schepler, and U. B. Ramabadran, "Improved Sellmeier coefficients for potassium titanyl arsenate $KTiOAsO_4$ (KTA)," paper TuW4, *OSA Ann. Meet.*, Dallas, TX, Oct. 2–7, 1994, and subsequent private communications.
[17] S. J. Brosnan and R. L. Byer, "Optical parametric oscillator threshold and linewidth studies," *J. Quantum Electron.*, vol. QE-15, pp. 415–431, 1979.
[18] L. K. Cheng, L. T. Cheng, F. C. Zumsteg, J. D. Bierlein, and J. Galperin, "Development of the nonlinear optical crystal $CsTiOAsO_4$ II. Crystal growth and characterization," *J. Crystal Growth*, vol. 132, pp. 289–296, 1993.
[19] K. Kato and M. Masutani, "Widely tunable 90° phasematched KTP parametric oscillator," *Opt. Lett.*, vol. 17, pp. 178–179, 1992.
[20] L. T. Cheng, L. K. Cheng, J. D. Bierlein, and F. C. Zumsteg, "Nonlinear optical and electrooptical properties of single crystal $CsTiOAsO_4$," *Appl. Phys. Lett.*, vol. 63, pp. 2618–2620, 1993.

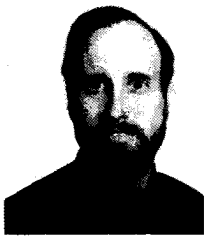

Glen A. Rines (M'90) was born in Rochester, NH, on Feb. 2, 1956. He received the B.A. degree in physics, from Gordon College, Wenham, MA, in 1977.

From 1978–1982 he worked in optical fiber technology, first at ITT Electro-Optics Products Division in Roanoke, VA, and then at Sanders Associates, in Nashua, NH. In 1982, he joined the laser systems department at Sanders Associates, where he worked primarily on the development of solid-state lasers in fluoride crystal hosts. Since 1985, he has been with Schwartz Electro-Optics, in Concord, MA. During this time, he has contributed to the development of a variety of solid-state laser systems, including diode laser pumped Nd lasers, cw and pulsed titanium sapphire lasers, and optical parametric oscillators.

Mr. Rines is a member of the Optical Society of America.

Henry H. Zenzie was born in Morristown, NJ, on April 10, 1962. He received the B.S. degree in physics, from Carnegie-Mellon University in 1983, and the M.S. degree in applied physics, from the Georgia Institute of Technology, in 1985.

From 1985 to 1990, he was employed by Sanders Associates, Nashua, NH, in the Laser Systems Department, where he participated in the development of diode-pumped lasers, mid-infrared optical parametric oscillators, and titanium sapphire lasers. Since joining the research division of Schwartz Electro-Optics, Concord, MA, in 1990, he has been involved in the development of solid-state lasers for medical applications.

Richard A. Schwarz (SM'83) was born in Weslaco, TX, on Sept. 30, 1967. He received the B.S. degree, in physics, from the Massachusetts Institute of Technology, Cambridge, MA, in 1990, and the M.S. degree, in optics, from the University of Rochester, Rochester, NY, in 1991.

From 1988–1989 he worked at the MIT Spectroscopy Laboratory in Cambridge, MA. During 1989–1990 he was with the Eye Research Institute, Boston, MA, working with a confocal scanning laser ophthalmoscope, for retinal studies. He joined the research division of Schwartz Electro-Optics (no relation), Concord, MA, in 1991, where he has contributed to the development of high energy, pulsed, injection seeded $Ti:Al_2O_3$ lasers, low threshold cw $Ti:Al_2O_3$ lasers, diode laser pumped Nd:YAG and Nd:YLF lasers, and Nd:YAG and Nd:YLF pumped optical parametric oscillators.

Yelena Isyanova was born in St. Petersburg, Russia. She received the Ph.D. degree in physics, from the Institute of Physics of the Belorussian Academy of Science, Minsk, USSR, in 1972.

From 1972 to 1991, she was employed as a senior research engineer, at the Leningrad Optics and Mechanics Association, Laser Division. Since 1992, she has been at the research division of Schwartz Electro-Optics. Through her R&D work, she has been involved in the development of solid-state and tunable lasers, and techniques for spatial and temporal laser parameter control.

Dr. Isyanova is a member of the Optical Society of America.

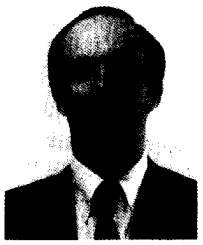

Peter F. Moulton (SM'84) was born in Springfield, MA, on May 27, 1946. He received the A.B. degree in physics, from Harvard College, Cambridge, MA, in 1968, and the M.S. and Ph.D. degrees, from the Department of Electrical Engineering and Computer Science, Massachusetts Institute of Technology, Cambridge, in 1971 and 1975, respectively.

He spent a postdoctorate year in 1975, at MIT Lincoln Laboratory, Lexington, MA, and became a staff member in 1976. His work at Lincoln Laboratory included high resolution, infrared spectroscopic measurements of molecules, development of lasers for remote sensing, and research and development of tunable and high efficiency solid-state lasers. Since 1985, he has been vice president and general manager of the research division of Schwartz Electro-Optics, Concord, MA, where he is engaged in the research and development of a new solid-state laser materials and systems. His areas of interest have included Ti:sapphire lasers, diode pumped lasers, mid infrared sources, parametric oscillators, medical applications of lasers and lidar systems.

Dr. Moulton is a Fellow of the Optical Society of America.